Aging effects on rheological properties of high viscosity modified asphalt

Article *in* Journal of Traffic and Transportation Engineering (English Edition) · March 2021

CITATIONS
5

READS
38

8 authors, including:

Wei Jiang
Chang'an University
66 PUBLICATIONS **1,054** CITATIONS
SEE PROFILE

Dongdong Yuan
Chang'an University
34 PUBLICATIONS **639** CITATIONS
SEE PROFILE

Zheng Lu Tong
Peking University
33 PUBLICATIONS **832** CITATIONS
SEE PROFILE

Aimin Sha
Chang'an University
186 PUBLICATIONS **2,041** CITATIONS
SEE PROFILE

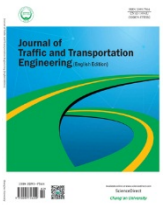

Journal of Traffic and Transportation Engineering(English Edition)
交通运输工程学报(英文)
ISSN 2095-7564,CN 61-1494/U

《Journal of Traffic and Transportation Engineering(English Edition)》网络首发论文

题目： Aging effects on rheological properties of high viscosity modified asphalt

作者： Wei Jiang，Dongdong Yuan，Zheng Tong，Aimin Sha，Jingjing Xiao，Meng Jia，Wanli Ye， Wentong Wang

网络首发日期： 2021-03-23

引用格式： Wei Jiang，Dongdong Yuan，Zheng Tong，Aimin Sha，Jingjing Xiao，Meng Jia，Wanli Ye，Wentong Wang. Aging effects on rheological properties of high viscosity modified asphalt ．Journal of Traffic and Transportation Engineering(English Edition). https://kns.cnki.net/kcms/detail/61.1494.U.20210322.0959.002.html

Published online：2021-03-23 11:13:29
URL：https://kns.cnki.net/kcms/detail/61.1494.U.20210322.0959.002.html

Aging effects on rheological properties of high viscosity modified asphalt

Wei Jiang[a, b]*, Dongdong Yuan[b*], Zheng Tong[b], Aimin Sha[a, b], Jingjing Xiao[c], Meng Jia[b], Wanli Ye[b], Wentong Wang[b]

[a]*Key Laboratory for Special Area Highway Engineering of Ministry of Education, Chang'an University, Xi'an 710064, PR China;*

[b]*School of Highway, Chang'an University, Xi'an 710064, RP China;*

[c]*School of Civil Engineering, Chang'an University, Xi'an 710064, PR China*

*Corresponding author: Wei Jiang, jiangwei_029@sina.com; Dongdong Yuan, ddy@chd.edu.cn

Highlights

- The effect of long-term aging on the viscoelastic properties of HVMA is higher than that of short-term aging.
- Aging improves the high-temperature property and reduces the low-temperature property of HVMA.
- The combination effect of neat asphalt binder and modifier causes the property changes of HVMA
- The anti-aging performance of HVMA exceeds the one of SK-90 and CRMA.

Abstract

This work investigated the aging effects on the rheological properties of high viscosity modified asphalt (HVMA). First, the high- and low-temperature rheological properties were measured by a dynamic shear rheometer and a bending beam rheometer, respectively. The aging mechanism was then tested using an Fourier transform infrared spectroscopy and a scanning electron microscope. Besides, a study was performed to compare the aging effects on the rheological properties of HVMA, crumb rubber modified asphalt

(CRMA), and neat asphalt (SK-90). The experimental results showed that the effects of the long-term aging on HVMA exceeded those of short-term aging. The complex shear modulus of the HVMA was improved by the aging in the whole frequency range. The complex shear modulus of the HVMA after the long-term aging was larger than after the short-term aging. Thus, the aging improved the high-temperature viscoelastic performance of HVMA. With a decrease in temperature from -12 °C to -24 °C, the low-temperature viscoelastic performance of HVMA decreased since its stiffness modulus and low continuous grading temperature increase. Both of the short- and long-term aging of HVMA were caused by an oxidation reaction, while modifier swelling also happened after long-term aging. Compared to CRMA and SK-90, aging had a limited influence on the high- and low-temperature rheological properties of HVMA.

Keywords:

High viscosity modified asphalt; Rheological properties; High-temperature; Low-temperature; Aging mechanism

1 Introduction

Asphalt ages during its production, transportation, construction, and service life (Cao et al., 2020; Ferrotti et al., 2018; Liu, X. et al., 2018; Wang, H. et al., 2020). Aging conditions of asphalt can be divided into two parts: short- and long-term aging (Osmari et al., 2019; Singh and Kumar, 2019). Aging happens in the mixing and paving processes is called short-term aging. Thin-film oven test (TFOT) and rolling thin film oven test (RTFOT) are two conventional methods to simulate short-term aging (Hofko et al., 2017; Jiang et al., 2020b; Jing et al., 2019b). In TFOT, 50 g of asphalt binder is put into a stainless-steel sample container. The thickness of the asphalt binder film is 3.2 mm. The test lasts for five hours at a rotary table rate of 5.5 r/min at 163 °C (ASTM, 2009). However, the TFOT has low reproducibility rates, and the effects of TFOTs various from one sample to another. For RTFTO, the test heats the asphaltic material in a rolling thin film oven for 85 minutes at 163 °C. The thickness of the asphalt binder (5-10 μm) in RTFTO approximates the thickness of the membrane in the asphalt

concrete. The aging conditions in the RTFOT tests are similar to the real mixing processes of asphalt concrete. Also, RTFOT keeps the modifier agitating during simulation, which avoids the segregation of modifier and asphalt binder. Compared with short-term aging, the aging during the service period is called long-term aging (Dhasmana et al., 2019). Pressurized aging vessel (PAV) is a widely-used and standard method for examining the effects of long-term aging (ASTM, 2013). In PAV, the aging temperature, aging time, and the container aeration pressure are 90-110℃, 20 h, and 2.1 MPa, respectively. Some existing studies have indicated that PAV was suitable to simulate the aging of asphalt binders in the first five years (Xu et al., 2016).

In recent years, many studies have used dynamic shear rheometers (DSRs) and bending beam rheometers (BBRs) to measure the rheological properties of asphalt after aging, such as time-temperature equivalent effects (Behera et al., 2013; Ye et al., 2019) and viscoelastic characteristics (Abdelmagid and Feng, 2019; Fu et al., 2019; Wu, 2017). Some studies tried to correlate the chemical and morphological composition of asphalt with its properties after aging (Hofko et al., 2017; Jing et al., 2019a). Many methods have been used to analyze the chemical and morphological changes of asphalt after aging, such as the use of Fourier transform-infrared spectroscopy (FT-IR) (Wang, F. et al., 2020), scanning electronic microscope (SEM) (Liu, H. et al., 2018; Singh and Kumar, 2019), gel permeation chromatography (GPC) (Hou et al., 2018), and atomic force microscope (AFM) (Yuan et al., 2020). Among these methods, FT-IR and SEM are efficient and convenient tools (Feng et al., 2016; Luo et al., 2020; Mazumder et al., 2018).

High viscosity modified asphalt (HVMA) is described by the concept of a type of asphalt whose dynamic viscosity exceeds 20,000 Pa·s (Chen et al., 2019). The scientific excitement about HVMA originates in the fact that it can significantly improve pavement performance (e.g., high-temperature stability and low-temperature crack resistance) because of its strong adhesion to aggregates (Hu et al., 2020; Jiang et al., 2018; Qin et al., 2018). Zhang et al. (Zhang and Hu, 2017; Zhang et al., 2018) studied the influence of plasticizer and crosslinker on the rheological properties. The results indicated that the plasticizer declined the rutting resistance of HVMA. Meanwhile, the crosslinker led to the formation of a polymer network, which improved the compatibility between the modifier and neat asphalt. Tan et al. and (Yourong et al., 2019) investigated the cohesion and adhesion of HVMA. The results showed that

the HVMA outperformed the neat asphalt binder on the cohesion at different temperatures. Besides, the cohesion of HVMA increased with an increase in the temperature. Compared to other modified asphalt binders, the HVMA had the best adhesion. Cai et al. (Cai, J. et al., 2019) prepared three new types of HVMA with waste materials, in which the experiments of pavement performance demonstrated the advantage of the new types of HVMA in temperature sensitivity, high-temperature properties, low-temperature properties, and storage stability. They concluded that crumb rubber powder, recycle oil and appropriate additives improved the performance of HVMA. In summary, many groups have made numerous contributions to the understanding of HVMA properties. However, there are few studies on HVMA aging.

Therefore, this work focuses on the aging effects on the rheological properties of HVMA. The high- and low-temperature rheological performance of the aged HVMA was first evaluated by DSR and BBR tests. An FT-IR and SEM were then used to investigate the aging mechanism of HVMA. Besides, a study was performed to compare the aging effects on the rheological properties of HVMA, crumb rubber modified asphalt (CRMA), and neat asphalt (SK-90). The main contribution of this study was the founds of differences between the effects of short- and long-term aging on the aging mechanism of HVMA. More precisely, the long-term aging of HVMA was postponed by the modifier swelling, while the short- and long-term aging of HVMA were both influenced by the oxidation reaction. The rest of the paper is organized as follows. Section 2 starts with describing the material preparation and the experimental details. Section 3 presents the experimental results and discussion. The conclusions are summarized in Section 4. Table 1 provides the abbreviations in the paper.

Table 1 Nomenclature of this study.

Abbreviation	Full name
HVMA	High viscosity modified asphalt binder
RTFOT	Rolling thin film oven test
PAV	Pressurized aging vessel
DSR	Dynamic shear rheometer
BBR	Bending beam rheometer
FT-IR	Fourier transform infrared
SEM	Scanning electron microscopy

TFOT	Thin-film oven test
SHRP	Strategic Highway Research Program
CRMA	Crumb rubber modified asphalt binder
SINOTPS-B	High viscosity modified asphalt modifier
VAI	Viscosity aging index
MSCR	Multiple stress creep recovery test
J_{nr}	Non-recoverable creep compliance
R	Percent recovery
$J_{nr\text{-}diff}$	Percent difference between J_{nr} at 0.1 kPa and 3.2 kPa
LT	Low-temperature continuous grading temperature
LTAI	Low-temperature continuous grading temperature aging index
CI	Denominator of the carbonyl functions index
SI	Sulfoxide functions index
CAI	Chemical aging index

2 Materials and methods

2.1 Raw materials

SK-90 neat asphalt (SK Holdings, South Korea) was used to prepare HVMA in this study. Table 2 and Table 3 presents the conventional properties of SK-90 and the high viscosity modified asphalt modifiers (SINOTPS-B), respectively.

Table 2 Conventional properties of SK-90.

Item	SK-90
Penetration at 25 °C, 0.1mm	97.1
Softening point, °C	47.4
Ductility at 5 °C, 5 cm·min^{-1}, cm	/
Viscosity at 60 °C by vacuum capillary viscometer, Pa·s	140.3

Table 3 Conventional properties of SINOTPS-B.

Item	SINOTPS-B
Particle size, mm	4
Density, g/cm^3	0.9
Water absorption rate,	0.3

2.2 *Sample preparations and tests*

As shown in Fig.1, the procedure of the sample preparations and tests can be summarized as follows. The HVMA was first prepared, as well as the CRMA and SK-90. The rheological properties of CRMA and SK-90 were used to compare to those of the HVMA. RTFOT and PAV were utilized to simulate the short- and long-term aging of HVMA, CRMA, and SK-90. DSR and BBR tests were performed to evaluate the high- and low-temperature viscoelastic properties of the three types of asphalt, respectively. An FT-IR and SEM were used to analyze the aging mechanism of the asphalt.

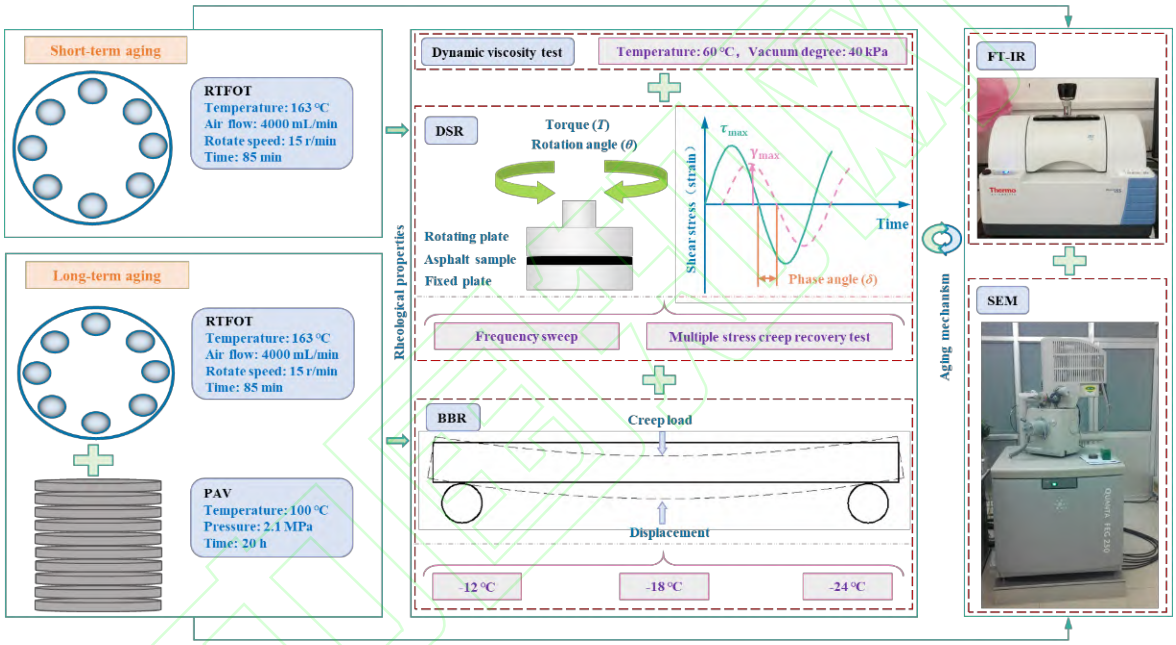

Fig.1 The flow chart of the research procedure

2.2.1 *Specimens preparation*

For the preparation of HVMA, the neat asphalt (SK-90) was first heated to 170 °C by a heating furnace. Then, the SINOTPS-B was added to the neat asphalt. The mass of the SINOTPS-B was 12% mass of the neat asphalt. Then, a FLUKO FM300 batch high shear was used to shear the mixture of neat asphalt and SINOTPS-B at 2,000 r/min for 10 min, afterward at 5,000 r/min for 30 min. Finally, the sheared mixture as HVMA was heated in the oven at 175 °C. The heating process lasted for 10 min. The SK-90 and CRMA were considered as the reference asphalts. Table 4 presents the conventional properties of

HVMA and CRMA.

Table 4 Conventional properties of HVMA and CRMA.

Item	HVMA	CRMA
Penetration at 25°C, 0.1mm	51.1	51.1
Softening point, °C	84.3	63.2
Ductility at 5°C, 5 cm·min^{-1}, cm	64.3	13.3
Viscosity at 60 °C by vacuum capillary viscometer, Pa·s	38696.9	3177.7

2.2.2 Laboratory aging

RTFOTs were conducted on the three kinds of asphalt (SK-90, CRMA, and HVMA) to simulate the short-term aging, according to ASTM D2872 (ASTM, 2012). Each type of the three asphalt was first heated to guarantee its flow ability. Then, the asphalt was poured into a glass container. Finally, the glass container was put into an SYD-0610 rolling thin-film oven for the simulation of short-term aging. The simulation time, temperature, rotation rate, airflow rate was 85 min, 163 °C, 15 r/min, 4000 mL/min, respectively.

PAV simulated the long-term aging following ASTM D6521 (ASTM, 2013). First, each type of the three asphalt binders was aged by a rolling thin-film oven. Second, residues after RTFOT were placed in a sample tray. Finally, the asphalt was aged in a Prentex 9500 PAV (100 °C, 2.1 MPa, 20 h).

2.2.3 Dynamic viscosity tests

Dynamic viscosity tests were conducted to measure the asphalt viscosity. A type of asphalt, whose viscosity is higher than 20,000 Pa·s, is defined as HVMA. In this study, a SYD-0620B type dynamic viscosity tester was used to measure the dynamic viscosities of asphalt binders. The test temperature and control vacuum were 60 °C and 40 kPa, respectively. The procedures of a dynamic viscosity test referred to ASTM D2171 (ASTM, 2010). The aging degree of the asphalt is characterized by a viscosity aging index (*VAI*) (Cai, X. et al., 2019; Mousavi et al., 2016) as

$$VAI=\frac{v_a-v_b}{v_b} \quad (1)$$

Here, v_a and v_b are the values of aged and unaged dynamic ~~viscosities~~ at 60 °C.

2.2.4 Dynamic shear rheometer (DSR) tests

In this study, a TA HR-2 DSR was used to measure the high-temperature properties of unaged and aged asphalt binders as follows.

(1) *Amplitude sweep test*. The amplitude sweep tests were used to determine the linear viscoelastic deformation limit of the asphalt binder. Fig.2 presents an example of the linear viscoelastic deformation limit of HVMA with a curve of complex shear modulus *G** vs. strain. The subsequent DSR tests were conducted based on the linear viscoelastic deformation limit. In this study, the strain amplitude was controlled at 1.0%.

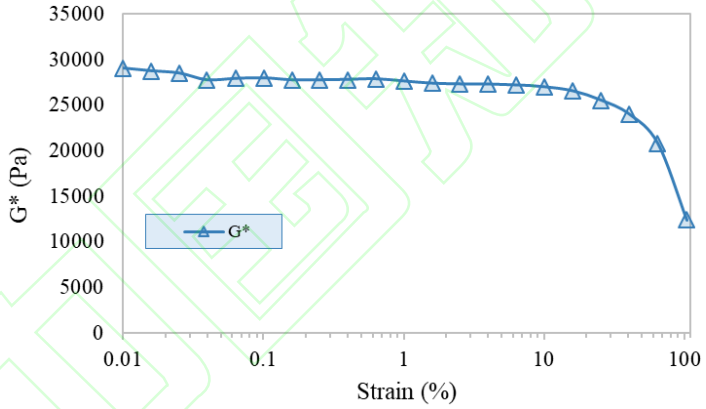

Fig.2 Linear viscoelastic deformation limit of HVMA.

(2) *Frequency sweep test*. In the study, the frequency sweep test was performed from 0.1 to 100 rad/s with five test temperatures (30 °C, 40 °C, 50 °C, 60 °C, 70 °C).

It is difficult to test the temperature and frequency changes of the asphalt accurately owing to the limitation of the current testing methods, such as the DSR test. Therefore, the modulus master curves were used to broaden the temperature and frequency range. The procedures to acquire the modulus master curves and the aging index (I_A) can be summarized as follows.

Step 1. Compute the shift factor α_T as

$$f'=\alpha_T \times f \quad (2)$$

and

$$\log \alpha_T = \frac{-C_1(T-T_1)}{C_2+T-T_1} \tag{3}$$

Here, f' and f are the conversion and unconversant load frequency (rad/s), respectively; α_T is the shift factor; $C_1 = 13$ and $C_2 = 112$ are empirical constants; T is the test temperature (°C); T_1 is the reference temperature (°C), which equal to 30 °C in this study.

Step 2. Fit a complex shear modulus master curve with a Sigmoidal function as (Gao et al., 2018; Jia et al., 2019)

$$\lg|G^*| = \eta + \frac{\alpha}{1+e^{\beta+\gamma(\lg f')}} \tag{4}$$

where G^* is the complex shear modulus (Pa); η is minimum modulus (Pa); α is the length value of modulus; β and γ are the shape parameters.

Step 3. Compute the area between the Sigmoidal function curves of the unaged and aged asphalt binders as

$$I_A = \int_{-3.5}^{2} \log G^*\left(\tilde{\xi}_{aged}\right) - \log G^*\left(\tilde{\xi}_{unaged}\right) \mathrm{d}\,\xi \tag{5}$$

Here, ξ is the logarithms of the diminished frequency among the integral limits (rad/s). The area was defined as an aging index (I_A) in a previous study (Cavalli et al., 2018; Xia et al., 2018).

(3) MSCR test. According to ASTM D7405 (ASTM, 2015), two creep stress levels (0.1 kPa and 3.2 kPa) were used for the MSCR tests. The two stress levels were carried out for 20 cycles and 10 cycles, respectively. Each cycle was divided into a creep phase of one second and a unloading recovery phase of nine seconds. The total duration is 300 s.

In the MSCR tests, non-recoverable creep compliance (J_{nr}), percentage of recovery (R), and percentage difference ($J_{nr\text{-}diff}$) were computed as (Stempihar et al., 2018)

$$J_{nr} = \frac{\varepsilon_u}{\sigma} \tag{6}$$

$$R = \frac{\varepsilon_p - \varepsilon_u}{\varepsilon_p} \tag{7}$$

$$J_{nr\text{-}diff} = \frac{J_{nr}(3.2) - J_{nr}(0.1)}{J_{nr}(0.1)} \tag{8}$$

where ε_u and ε_p are the unrecoverable strain (%) and the peak strain (%), respectively; σ is the loading

stress (Pa); and J_{nr}(3.2) and J_{nr}(0.1) are the values of J_{nr} under 3.2 kPa and 0.1 kPa, respectively. The high-temperature rutting phenomenon is evaluated by the value of J_{nr}, and R indicates the ability to restore from deformation in a specific recovery time; $J_{nr\text{-}diff}$ measures the relative difference of irrecoverable creep compliances under 3.2 kPa and 0.1 kPa.

2.2.5 Bending beam rheometer (BBR) tests

In BBR tests, three test temperatures (-12°C, -18°C and -24°C) were selected to evaluate the low-temperature performance of the three asphalt binders. The deflection in the middle of the beam under a load of 980 mN was measured. The creep stiffness and *m*-value, respectively, were then calculated as

$$S(t)=\frac{Pl^3}{4bh^3\delta(t)} \tag{9}$$

$$m=d\lg S(t)/d\lg t \tag{10}$$

Here, $S(t)$ is the stiffness modulus at the t-moment (MPa); m is creep rate; P is an applied constant load (980 mN); and l=102.0mm, b=12.7mm, h=6.25mm are the length, width, height of an asphalt beam, respectively; $\delta(t)$ is the center deflection of the asphalt beam at the t-moment (mm).

The creep stiffness and *m*-value were used to calculate the low-temperature continuous grading temperature (LT). The LT of creep stiffness (LT_S) was calculated as

$$LT_S=T_1+\left(\frac{\log_{10}(P_S)-\log_{10}(P_1)}{\log_{10}(P_2)-\log_{10}(P_1)}\right)(T_2-T_1) \tag{11}$$

and the LT of *m*-value (LT_m) was calculated as

$$LT_m=T_1+\left(\frac{P_S-P_1}{P_2-P_1}\right)(T_2-T_1) \tag{12}$$

Here, LT_S and LT_m is calculated by the creep stiffness and m-value, respectively, (°C); and P_S is equal to 300 MPa. The final value of LT is the maximum value between LT_S and LT_m. The aging degree of asphalt can be characterized by an LT aging index ($LTAI$) as

$$LTAI=\frac{(LT)_{of\ unaged}-(LT)_{of\ aged}}{(LT)_{of\ unaged}} \tag{13}$$

2.2.6 Aging mechanism tests

(1) *Fourier transform infrared (FT-IR) test.* A portable Fourier transform infrared spectrometer Thermo Scientific Nicolet iS5 was utilized to analyze the chemical changes of the asphalt in this study. The wavenumber range was 650 cm^{-1}- 4,000 cm^{-1} with a 4 cm^{-1} resolution. The number of scanning was 32 times, and the attenuated total reflectance with crystal ZnSe was used for the spectrum collection. The peak area ratios were then calculated based on Lambert-Beer's law (Sun et al., 2011). Finally, the changes in the peak area ratios between the unaged and aged asphalt were used to characterize the aging degree. Additionally, carbonyl function index (*CI*) and sulfoxide function index (*SI*) (Hu et al., 2018; Jiang et al., 2020a; Marsac et al., 2014; Wang et al., 2018), as two metrics for the evaluation of chemical aging, can be expressed as

$$CI = \frac{V(\approx 1{,}700)}{V(v_{ref})} \tag{14}$$

$$SI = \frac{V(\approx 1{,}030)}{V(v_{ref})} \tag{15}$$

where $V(v_{ref})$ is the peak area in 1,376 cm^{-1}- 1,455 cm−1, V(≈1,700) and V(≈1,030) are the peak areas of 1700 cm^{-1} and 1,030 cm^{-1}, respectively. The sum of *CI* and *SI* is defined as the chemical aging index (*CAI*) (Cavalli et al., 2018; Mousavi et al., 2016).

(2) *Scanning electron microscopy (SEM) test***.** An SEM (FEI Quanta FEG250 scanning electron microscope) was utilized to observe the morphological changes of HVMA after aging. In SEM, it is used to bombard the sample surface with a fine focusing an electron beam under the vacuum state. And the secondary electrons are used to generate the image on the computer screen. In the preparation of SEM test samples, the asphalt was first heated to the molten state and mixed evenly. Then, asphalt samples were scraped a thin layer on the test bench with a scraper. Moreover, the asphalt sample was sprayed with gold for 15 s at 40 mA in a fully automatic magnetron ion sputtering apparatus owing to the non-conductivity of asphalt.

3 Results and discussion

3.1 Rheological test analysis

3.1.1 Dynamic viscosity tests

Fig.3 shows the dynamic viscosities of SK-90, HVMA, and CRMA. The dynamic viscosities of SK-90, HVMA, and CRMA before the short-term aging was 1.2, 0.1, and 1.1 times after the short-term aging, respectively. The dynamic viscosities of the three-asphalt increased 12.4, 2.1, and 10.9 times after the long-term aging. This was because the light components in the asphalt were volatilized, and a part of the small molecules converted to the macromolecules. Therefore, the average molecular weights of the three types of asphalt increased, which led to an increase in the dynamic viscosities.

The *VAI*s of the three types of asphalt are presented in Fig.4. The *VAI*s of the three asphalt after short-term aging is smaller than after long-term aging. Thus, the effects of short-term aging on the dynamic viscosity were not as significant as those of long-term aging. After both short- and long-term aging, the *VAIs* of the HVMA is the minimum. Therefore, the HVMA has the optimal anti-aging property among the three types of asphalt.

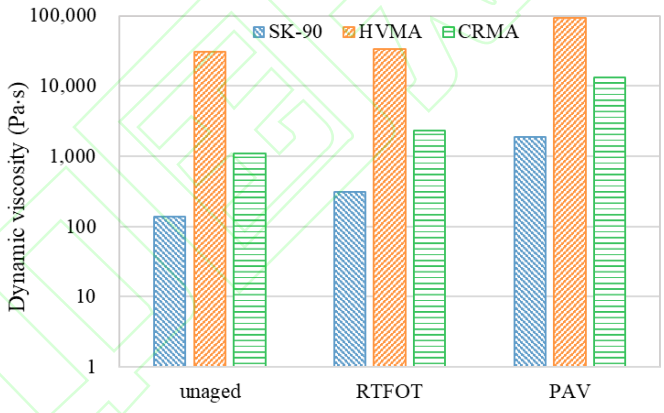

Fig.3 Asphalt dynamic viscosity at 60 ℃.

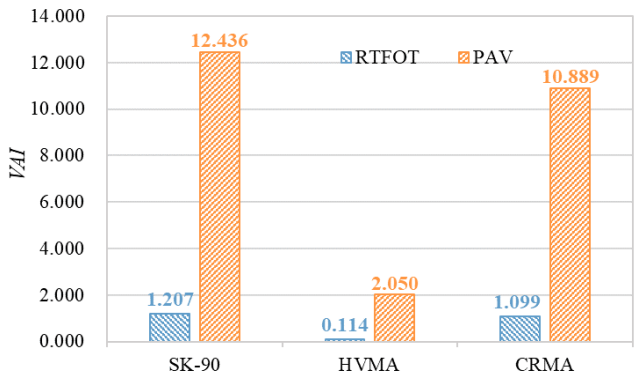

Fig.4 Viscosity aging index of three kinds of asphalt

3.1.2 Aging effects on high-temperature rheological properties

(1) *Frequency sweep tests analysis*.

Fig.5 presents the complex shear modulus master curves of the SK-90, HVMA and CRMA. The complex shear modulus of the SK-90, HVMA, and CRMA increased with an increase in frequency. This was because there were the lag processes of asphalt in response to the load. The asphalt was not able to deform instantaneously at the moment of loading or unloading. Therefore, the accumulated energy of the loading stress was not released immediately.

Fig.5 also demonstrated that there were $|G^*_{PAV}| > |G^*_{RTFOT}| > |G^*_{unaged}|$ in the whole frequency range for SK-90, HVMA, and CRMA. This indicated that the aging effect improved the deformation resistance of asphalt, which was mainly due to the transformation of asphalt components. Some light components of the asphalt binders were transferred into the heavy components. The transformation made the asphalt stiffen.

The complex shear modulus of SK-90, HVMA, and CRMA after short- and long-term aging were close at the high-frequency stage (Fig.5). However, at the low-frequency stage, the complex shear modulus of each type of the asphalts after long-term aging was larger than that after short-term aging. As the time-temperature equivalent, a low-frequency stage stands for a high-temperature condition. Thus, the high-temperature rheological properties of the asphalt increased after aging. Compared to short-term aging, long-term aging had more significant effects on the asphalt.

According to Eq. (5), the I_A results of the three types of asphalt were calculated, as shown in Fig.6. The value of I_A after long-term aging was larger than after short-term aging. This indicated that long-term aging had more significant effects than short-term aging. After aging, compared to CRMA and SK-90, HVMA had the desirable anti-aging ability as I_A (SK-90) $>$ I_A (CRMA) $>$ I_A (HVMA).

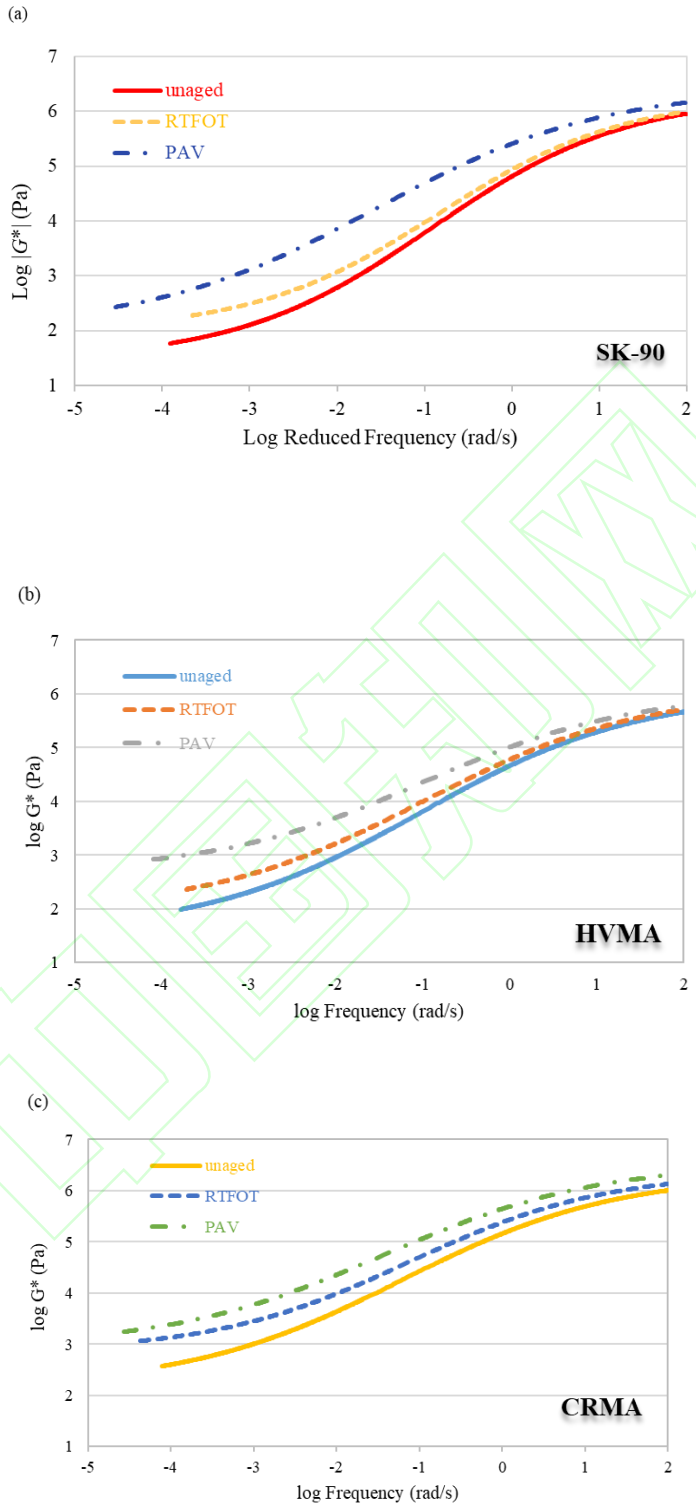

Fig.5 Complex shear modulus master curve: (a) SK-90; (b) HVMA; (c) CRMA

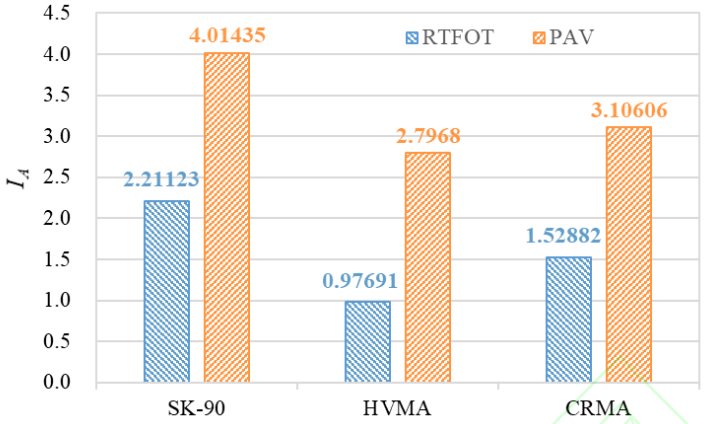

Fig.6 Modulus master curves aging index of three types of asphalt

(2) MSCR tests analysis

Fig.7 presents the strain responses of the SK-90, HVMA, CRMA. The strain levels, as responses to stress, increased at specified stress levels. Thus, the curves had obvious creep recovery stages. The curves of the HVMA and CRMA showed an exponential growth type. With an increase in the recovery time, the delayed elastic deformation continuously recovered in the HVMA and CRMA. However, the deformation recovery of the SK-90 did not continue with the increase in time. In the recovery stage, the three kinds of asphalt had no fully elastic recovery, as shown in Fig.7.The HVMA and CRMA showed delayed elastic deformation in the creep phase, but the deformation of the SK-90 did not restore permanently after unloading.

After aging, all three kinds of asphalt had small deformations and poor recovery abilities at a certain stress level. This indicated that aging had negative effects on the recovery abilities of the asphalt binders. For the HVMA, the recovery abilities after long-term aging outperformed that after short-term aging. This was because the swelling effects of the high viscosity modifiers decreased after long-term aging, which led to the reconstitution of the small particles in the HVMA under the thermal oxidation. The reconstitution improved the recovery abilities of the HVMA.

In Fig.8 (a) and (b), there are J_{nr} (3.2) > J_{nr} (0.1) and R (3.2) < R (0.1) for all of the three asphalt binders. Thus, the rutting resistance and recovery ability decreased with an increase in the stress. This was because of the stress sensitivity of asphalt binders, in which the increase in the stress improve the viscous components of each asphalt, as well as the decrease in the elastic component. The values of

J_{nr} and R in the HVMA was the minimum and maximum, respectively. This indicated that the rutting resistance and recovery ability of the HVMA was optimal.

After aging, J_{nr}'s values in the three types of asphalt decreased, but R increased, as shown in Fig.8. This indicated the aging improved the rutting resistance and the recovery ability, which was due to the hardening and brittleness of the asphalt. Besides, the long-term aging had lower J_{nr} and higher R than the short-term aging. This demonstrated that the effect of long-term aging outweighed that of short-term one.

In Fig.8 (c), the value of $J_{nr\text{-}diff}$ in the HVMA and CRMA decreased after aging, which demonstrated the decrease in the stress sensitivity of the two asphalt binders after aging. This was because that the aging led to the small-particle reconstitution and sub-structure change in the modifier. As for the SK-90, the values of $J_{nr\text{-}diff}$ increased after short-term aging but decreased after long-term aging. This might be owing to the effects of repeating creep loads and aging.

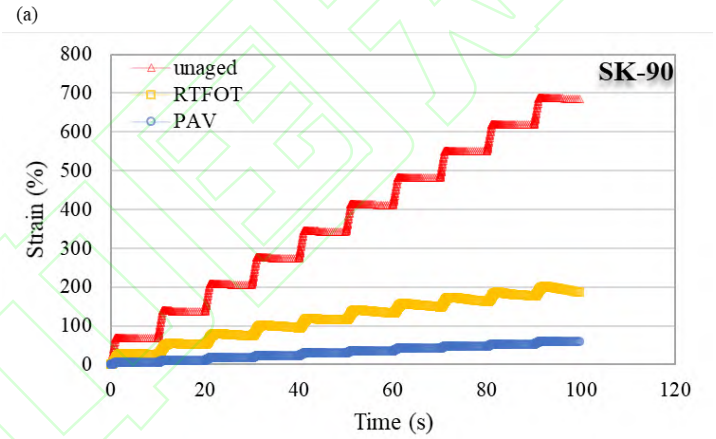

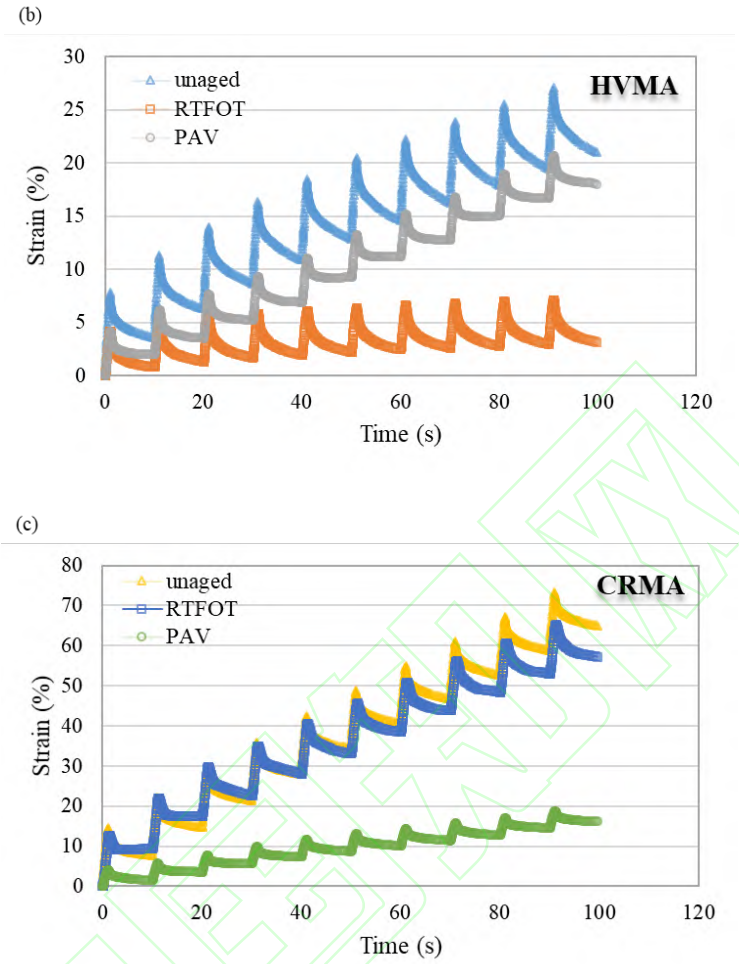

Fig.7 Shear strain at 0.1 kPa: (a) SK-90; (b) HVMA; (c) CRMA

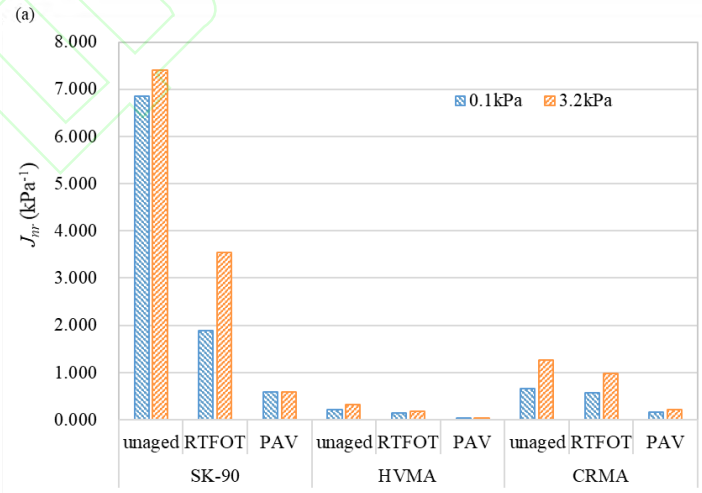

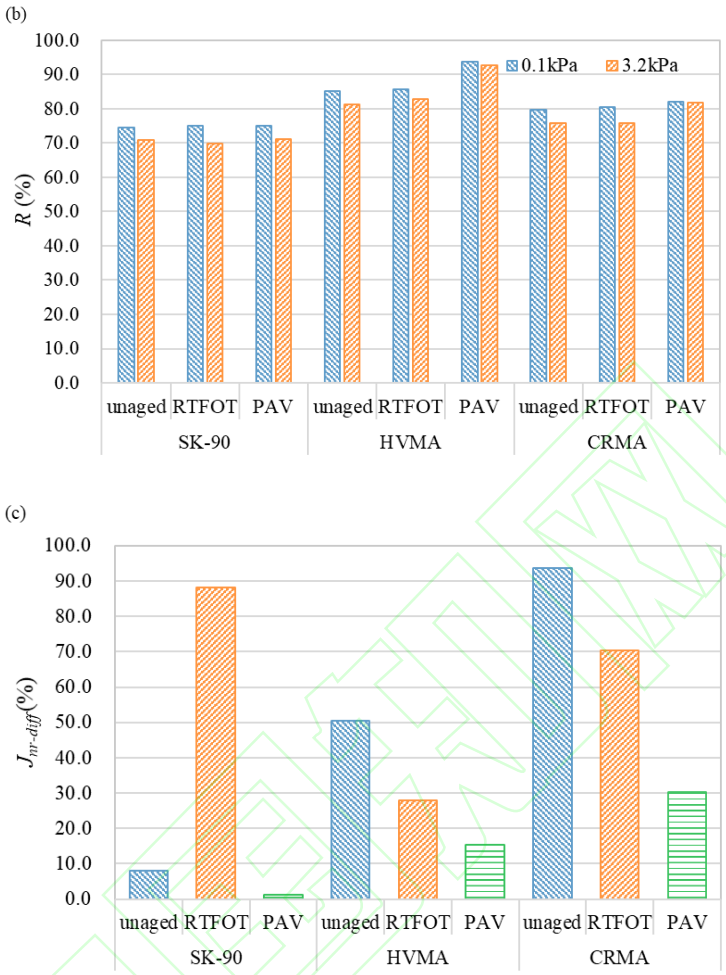

Fig.8 MSCR parameters of different kinds of asphalt: (a) average non-recoverable creep compliance; (b) average percent recovery; (c) percent difference between *Jnr* (0.1) and *Jnr* (3.2)

3.1.3 Aging effects on high-temperature rheological properties

(1) *Low-temperature flexural creep stiffness*

Fig.9 presents the low-temperature stiffness modulus with the change of the loading time. The stiffness modulus of the SK-90, HVMA, and CRMA was close with the change of the loading time. The stiffness modulus decreased with an increase in the loading time. The change rates are illustrated in Table 5. The temperature of -12 °C had the largest effect on the stiffness modulus, followed by the temperature of -18 °C and -24 °C. Thus, a low temperature had a limited influence on the stiffness modulus. Table 5 also showed that the change rate of stiffness modulus decreased after aging. The change rate of

long-term aging is smaller than that of short-term aging, indicating that the effect of long-term aging is greater than that of short-term aging on the stiffness modulus. However, the change rates of stiffness modulus in the three asphalt binders were different. This might be due to the four-components of asphalt (saturates, aromatics, resins, and asphaltenes) impact the low-temperature property and aging property of asphalt, and the content of the four-components will also change with the modification and aging of asphalt.

(a)

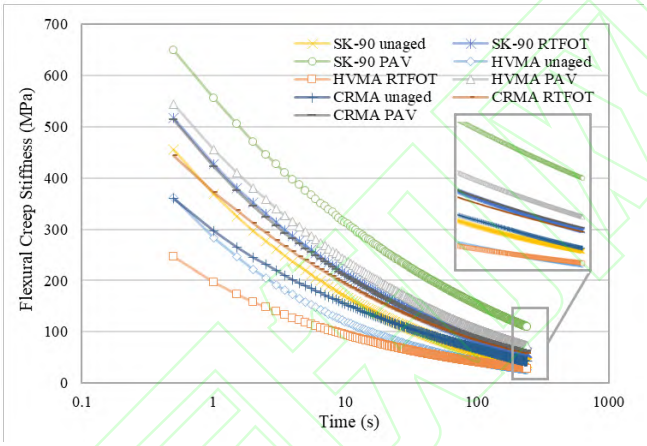

(b)

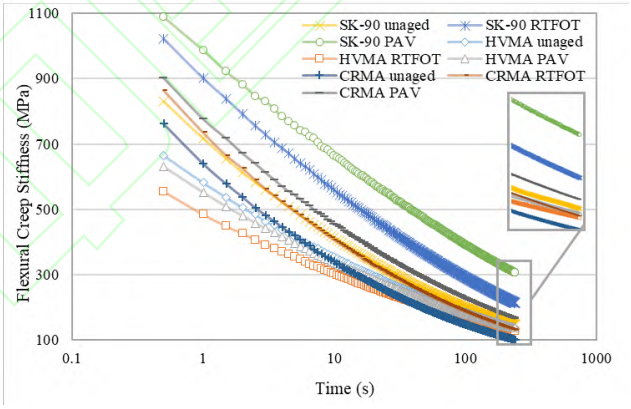

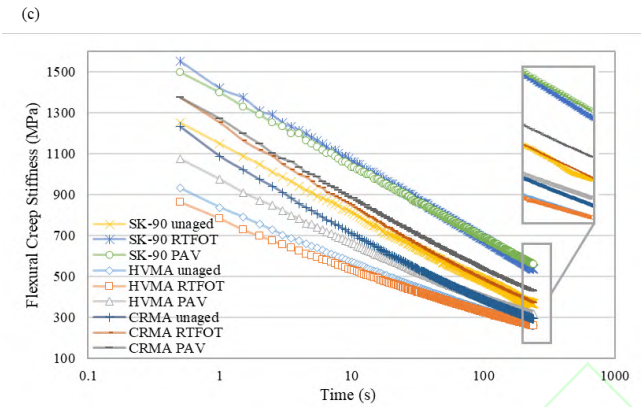

Fig.9 Relationship between flexural creep stiffness and loading time: (a) -12 ℃; (b)-18 ℃; (c) -24 ℃.

Table 5 Change rates of flexural creep stiffness.

Samples		-12℃	-18℃	-24℃
SK-90	Unaged	91.4%	82.3%	70.6%
	RTFOT	88.6%	79.1%	65.4%
	PAV	83.1%	71.9%	62.7%
HVMA	Unaged	92.8%	79.6%	72.0%
	RTFOT	88.6%	78.4%	70.6%
	PAV	86.7%	77.2%	69.9%
CRMA	Unaged	88.2%	86.8%	76.1%
	RTFOT	88.0%	84.9%	73.0%
	PAV	87.9%	81.5%	68.7%

(2) Low-temperature continuous grades

Fig.10 shows the BBR test results of the SK-90, HVMA, and CRMA under different aging conditions. The stiffness moduli of the three types of asphalt increased, but the creep rates decreased after aging. In the study, *LT* was also used to evaluate the low-temperature performance of aged asphalt. As shown in Fig.11, the *LT*s of the three asphalt binders increased after both short- and long-term aging. This was because the aging decreased the oil contents (aromatics and saturation) and increased the proportion of asphaltene, which reduced the plasticity and ductility of asphalt binders.

Fig.11 presents the *LT* of HVMA is larger than that of CRMA. This was because the modifiers particles decomposed when HVMA and CRMA were prepared. However, the rubber in the CRMA only swelled during the preparation process. The SINOTPS-B in the HVMA both swelled and cross-linked during the

preparation processes. This led to the desirable low-temperature performance of HVMA. Additionally, the increase in the values of *LT* in the HVMA was the smallest in the three asphalt binders after both short- and long-term aging. This indicated that the HVMA outperformed the CRMA and SK-90 on the anti-aging properties.

Fig.12 presents the *LTAI* results of the three kinds of asphalt. The *LTAI*s of the SK-90, HVMA, CRMA after short-term aging were all less than those after long-term aging. This indicated that the effects of short-term aging on *LTAI* were less than the ones of long-term aging. After aging, the *LTAI* of the HVMA was the minimum. Thus, the aging resistance of HVMA exceeded those of CRMA and SK-90.

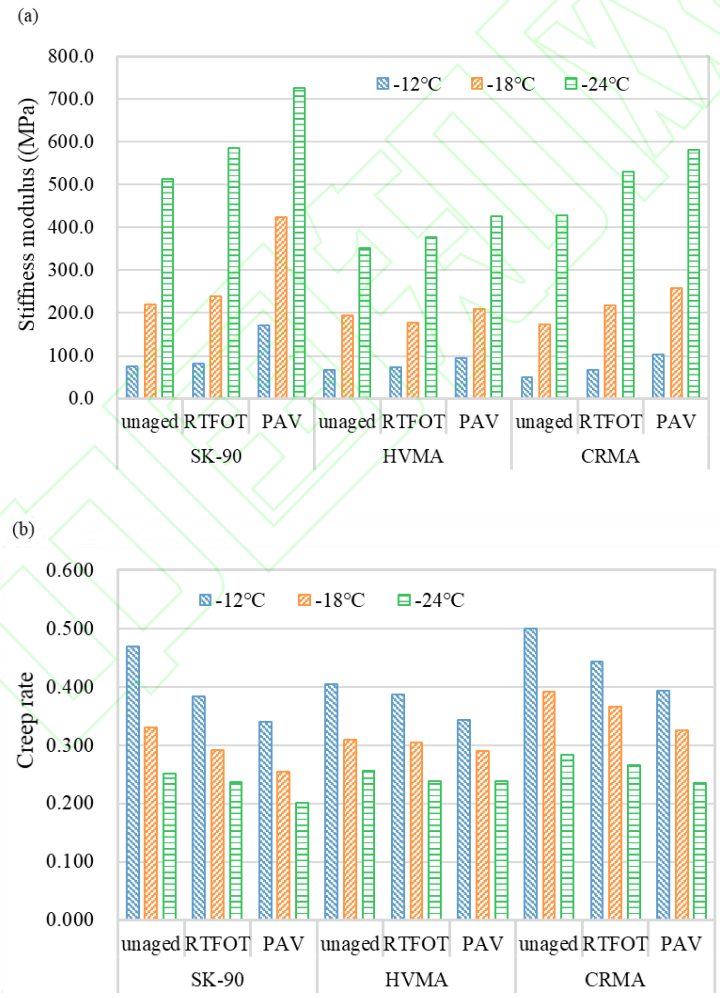

Fig.10 BBR test results under different aging conditions: (a) stiffness modulus; (b) m-values.

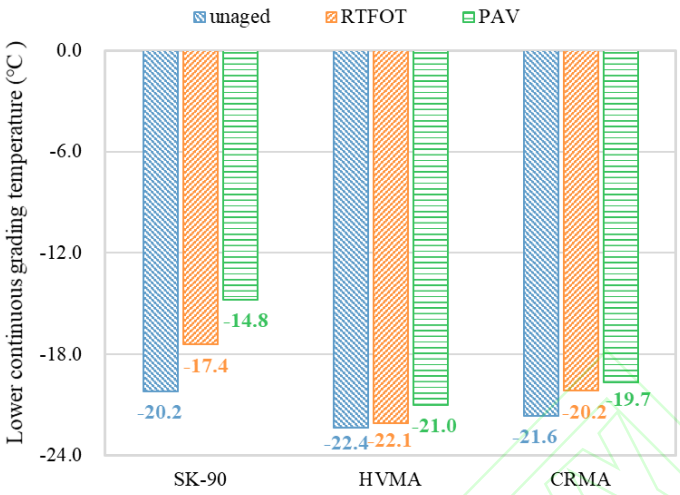

Fig.11 Continuous grades temperature

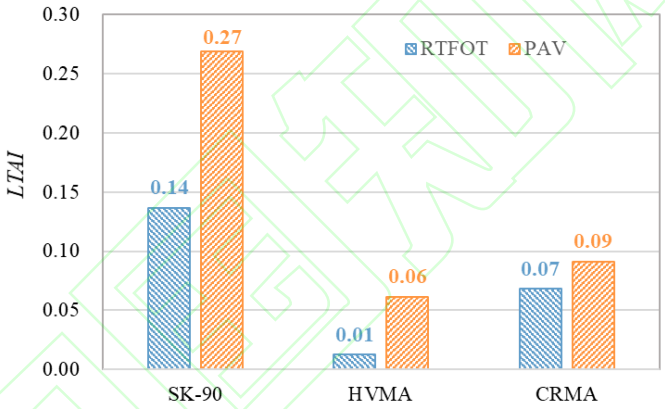

Fig.12 Low-temperature continuous grading temperature aging index of three asphalt binders

3.2 Aging mechanism analysis by FT-IR and SEM

FT-IR is an efficient method to analyze the chemical functional groups of asphalt binders (Wang, W. et al., 2020). Fig.13 showed the FT-IR spectrum of SK-90, HVMA, CRMA at different aging conditions. The characteristic peaks within 774-836 cm^{-1} represent the stretching vibration of S-O. The bending vibration peak of olefin (CH) is at 941-981 cm^{-1}. The stretching vibration within 980-1145 cm^{-1} represents alcohols (C-OH). The characteristic peaks within 1238-1280 cm^{-1} stand for the stretching vibration of C-O-C, indicating the existence of epoxy propane in the asphalt. The peak at 1351-1489 cm^{-1} is the variable angle vibration peak. The stretching vibration peak within 1556-1598 cm^{-1} demonstrates the existence of olefin. The peak at 1713 cm^{-1} indicates the stretching vibration of C=O. The peaks within 2878-2978

cm^{-1} are considered as the $-CH_2$ stretching vibration. The stretching vibration of the -OH group in the binder molecules should be observed at 3200-3500 cm^{-1}.

In Fig. 13(a), the unaged HVMA and CRMA exhibited the vibration peaks at 774-836 cm^{-1}, 941-981 cm^{-1}, 980-1145 cm^{-1}, 1238-1280 cm^{-1}, and 3200-3500 cm^{-1}. This indicated that in the process of preparing HVMA and CRMA formed some functional groups, such as S-O, CH, C-OH, C-O-C, -OH.

After short-term aging (Fig.13(b)), the stretching vibration of the -OH group (3200-3500 cm^{-1}) of the three asphalt binders was close. This indicated that the short-term aging of three asphalt binders is accompanied by oxygenation. The HVMA had the strongest absorption peak at 774-836 cm^{-1}, 980-1145 cm^{-1}, 1351-1489 cm^{-1}, 1556-1598 cm^{-1}, 2878-2978 cm^{-1}, followed by CRMA and SK-90. However, the values of these peaks in the CRMA were larger than those in the HVMA after long-term aging. This might be the swelling of crumb rubber was generally weakened and the oxidation of asphalt was intensified. Additionally, there were obvious absorption peaks at 1713 cm^{-1} after both short- and long-term aging, which indicated the obvious existence of oxidation reaction in the three asphalts.

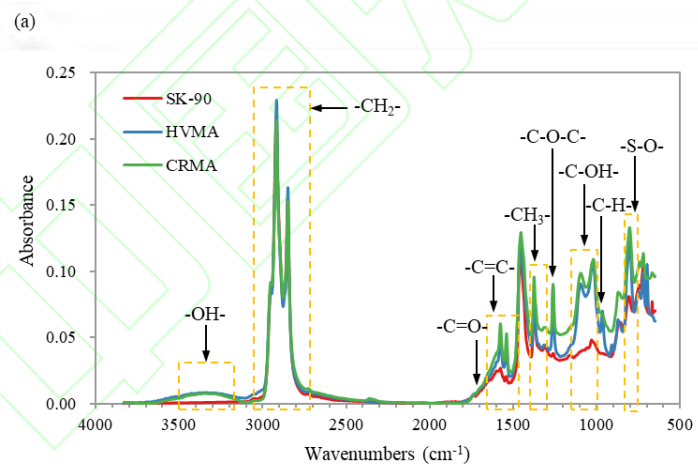

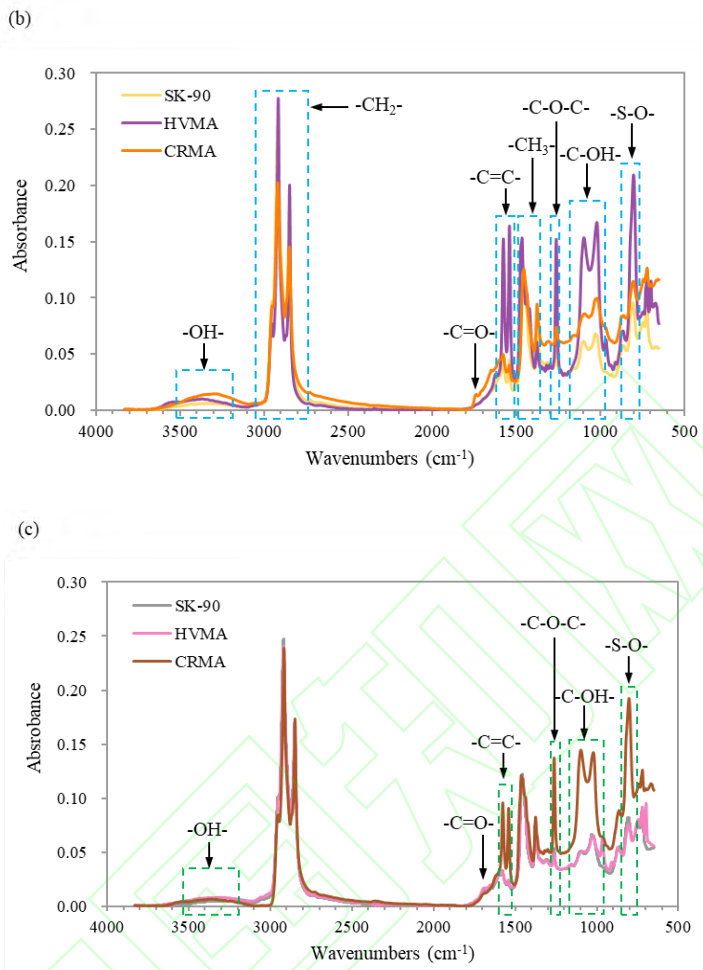

Fig.13 FT-IR spectra of asphalt: (a) unaged; (b) RTFOT; (c) PAV.

Fig.14 presents the *CAI* results of the three asphalt binders based on the infrared spectra in Fig.13. The *CAI* of three asphalt binders increased after aging. This indicated that there was an accumulation of oxidation reaction in the three kinds of asphalt during aging. After short-term aging, the *CAI* growth rate of SK-90, HVMA, and CRMA was 54.9%, 143.8%, and 12.5%, respectively. This indicating that the short-term aging had the most significant effect on HVMA, followed by SK-90 and CRMA. The long-term aging had the largest effect on SK-90, followed by CRMA and HVMA. The *CAI* growth rate of SK-90, HVMA, and CRMA was 81.9%, 38.2%, and 42.8%.

The change of *CAI* in the HVMA was different from that of SK-90 and CRMA. The *CAI* of short-term aging larger than that of long-term aging. This might be because the swelling effect of the SINOTPS-B modifiers modifier is much greater than the oxidation reaction after long-term aging.

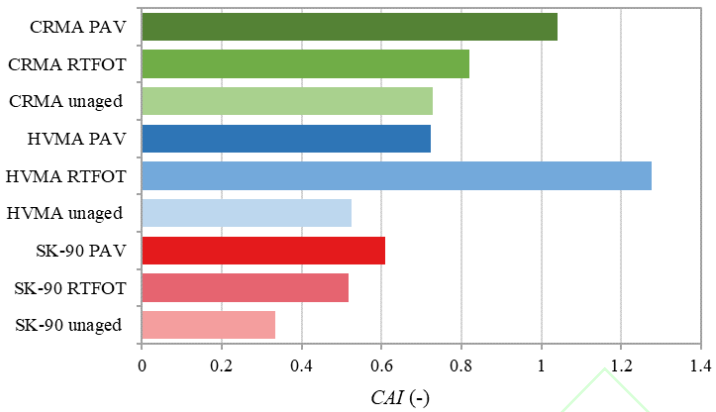

Fig.14 Chemical aging index of three asphalt binders.

Fig.15 shows the SEM images of the SK-90, HVMA, and CRMA. The network structures of HVMA and CRMA can be found in Fig.15(d)-(i). The structures were generated with the infiltration and diffusion of the light components in the neat asphalt binder into the SINOTPS-B modifiers and crumb rubber modifiers during the processes of mixing and blending. These network structures continuously disappeared during aging, such as shown from Fig. 15(d) to Fig. 15(f). This indicated that the contents of small molecules decreased, and the contents of large molecules increased after aging, which led to the asphalts stiffen. The influence of long-term aging was more obvious than that of short-term aging since the network structures after long-term aging was less obvious than those after short-term aging.

Fig.15 (e) and Fig.15 (f) show the SEM images of HVMA after short- and long-term aging, respectively. The SINOTPS-B modifiers degraded into an unstable phase, which led to an asphalt rich phase with some segregated polymer patches. After long-term aging, the SINOTPS-B modifiers were further degraded, in which there were few modifiers in the asphalt. Thus, the interface areas between the SINOTPS-B modifiers and asphalt binder were reduced. A similar phenomenon was also found in the CRMA.

(a) (b) (c)

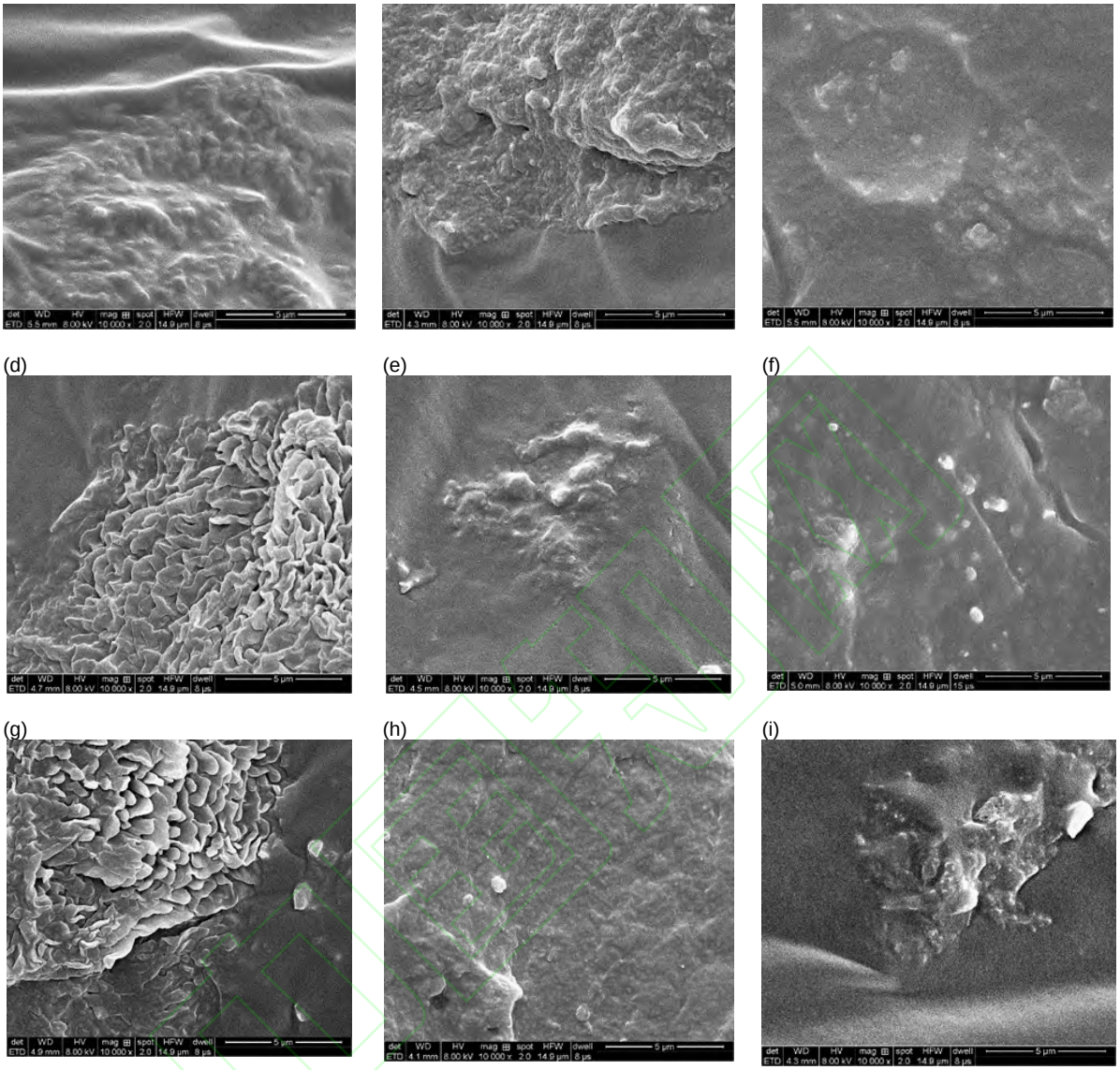

Fig.15 SEM photos of asphalt binders (10 000x): (a) SK-90-unaged; (b) SK-90-RTFOT; (c) SK-90-PAV; (d) HVMA-unaged; (e) HVMA-RTFOT; (f) HVMA-PAV; (g) CRMA-unaged; (h) CRMA-RTFOT; (i) CRMA-PAV.

4 Conclusions

A study of the aging effects on HVMA is presented and the main conclusions can be summarized as follows:

(1) In the evaluation of the high-temperature performance, the dynamic viscosity and complex shear modulus of HVMA were stable and desirable after the short- and long-term aging. The complex shear modulus of the HVMA was improved by the aging in the whole frequency range. The effects of

short-term aging are less than those of long-term aging. Additionally, the HVMA had good adaptability to stress change and low-stress sensitivity after aging.

(2) After aging, the low-temperature stiffness modulus and low continuous grading temperature of the HVMA increased. Compared with the CRMA and SK-90, the HVMA had the maximum *LT* both before and after aging. The short- and long-term aging have little effect on the low-temperature property of HVMA.

(3) The aging mechanism of the HVMA was different between the short- and long-term aging. The short-term aging mainly depended on the oxidation reaction. However, the long-term aging was affected by both the oxidation reaction and the modifier swelling.

Acknowledgements

This project was jointly supported by the National Key R&D Program of China (Grant No. 2018YFB1600200), the Fok Ying-Tong Education Foundation (Grant No. 161072), the Youth Top-notch Talent Support Program of Shaanxi Province, and the Fundamental Research Funds for the Central Universities (Grant No. 300102219317). The writers express they are thanks to Aboudou Wassiou Ogbon of Chang'an University for his language assistance.

Conflict of interest

The authors do not have any conflict of interest with other entities or researchers.

References

Abdelmagid, A.A.A., Feng, C.P., 2019. Laboratory evaluation of the effects of short-term aging on high temperature performance of asphalt binder modified with crumb rubber and rice husk ash. Petrol Sci Technol 37(13), 1557-1565.

ASTM, 2010. Standard test method for viscosity of asphalts by vacuum capillary viscometer. Annual Book of Standards.

ASTM, 2012. Standard test method for effect of heat and air on a moving film of asphalt (rolling thin-film oven test), ASTM D2872. West Conshohocken, PA.

ASTM, 2013. Standard practice for accelerated aging of asphalt binder using a pressurized aging vessel (PAV), ASTM D6521. Westen Conshohocken, PA.

ASTM, 2015. Standard Test Method for Multiple Stress Creep and Recovery (MSCR) of Asphalt Binder Using a Dynamic Shear Rheometer, ASTM D7405. West Conshohocken, PA.

ASTM, D., 2009. Standard test method for effects of heat and air on asphaltic materials (thin-film oven test). Annual book of ASTM standards 4.
Behera, P.K., Singh, A., Amaranatha Reddy, M., 2013. An alternative method for short-and long-term ageing for bitumen binders. Road Mater Pavement 14(2), 445-457.
Cai, J., Song, C., Zhou, B., Tian, Y., Li, R., Zhang, J., Pei, J., 2019. Investigation on high-viscosity asphalt binder for permeable asphalt concrete with waste materials. J Clean Prod 228, 40-51.
Cai, X., Zhang, J.Y., Xu, G., Gong, M.H., Chen, X.H., Yang, J., 2019. Internal aging indexes to characterize the aging behavior of two bio-rejuvenated asphalts. J Clean Prod 220, 1231-1238.
Cao, Y., Sha, A., Liu, Z., Li, J., Jiang, W., 2020. Energy output of piezoelectric transducers and pavements under simulated traffic load. Journal of Cleaner Production 279, 123508.
Cavalli, M.C., Zaumanis, M., Mazza, E., Partl, M.N., Poulikakos, L.D., 2018. Effect of ageing on the mechanical and chemical properties of binder from RAP treated with bio-based rejuvenators. Composites Part B: Engineering 141, 174-181.
Chen, X., Li, C., Jiang, Y., Zhang, W.G., Xu, G.J., 2019. Comparisons with high viscosity additive effects on base and modified asphalt. Petrol Sci Technol 37(11), 1331-1337.
Dhasmana, H., Hossain, K., Karakas, A.S., 2019. Effect of long-term ageing on the rheological properties of rejuvenated asphalt binder. Road Mater Pavement, 1-19.
Feng, Z.-g., Bian, H.-j., Li, X.-j., Yu, J.-y., 2016. FTIR analysis of UV aging on bitumen and its fractions. Mater Struct 49(4), 1381-1389.
Ferrotti, G., Baaj, H., Besamusca, J., Bocci, M., Cannone-Falchetto, A., Grenfell, J., Hofko, B., Porot, L., Poulikakos, L., You, Z., 2018. Comparison between bitumen aged in laboratory and recovered from HMA and WMA lab mixtures. Mater Struct 51(6), 150.
Fu, Q.H., Xu, G., Chen, X.H., Zhou, J., Sun, F.M., 2019. Rheological properties of SBS/CR-C composite modified asphalt binders in different aging conditions. Constr Build Mater 215, 1-8.
Gao, J., Wang, H., You, Z., Hasan, M.R.M., 2018. Research on properties of bio-asphalt binders based on time and frequency sweep test. Constr Build Mater 160, 786-793.
Hofko, B., Cannone Falchetto, A., Grenfell, J., Huber, L., Lu, X., Porot, L., Poulikakos, L., You, Z., 2017. Effect of short-term ageing temperature on bitumen properties. Road Mater Pavement 18(sup2), 108-117.
Hou, X., Xiao, F., Wang, J., Amirkhanian, S., 2018. Identification of asphalt aging characterization by spectrophotometry technique. Fuel 226, 230-239.
Hu, J., Wu, S., Liu, Q., Hernández, M.I.G., Zeng, W., 2018. Effect of ultraviolet radiation on bitumen by different ageing procedures. Constr Build Mater 163, 73-79.
Hu, M., Sun, G., Sun, D., Zhang, Y., Ma, J., Lu, T., 2020. Effect of thermal aging on high viscosity modified asphalt binder: Rheological property, chemical composition and phase morphology. Constr Build Mater 241, 118023.
Jia, M., Sha, A., Zhang, Z., Li, J., Yuan, D., Jiang, W., 2019. Effect of organic reagents on high temperature rheological characteristics of organic rectorite modified asphalt. Constr Build Mater 227, 116624.
Jiang, W., Huang, Y., Sha, A.M., 2018. A review of eco-friendly functional road materials. Constr Build Mater 191, 1082-1092.
Jiang, W., Li, P., Ye, W., Shan, J., Li, Y., Xiao, J., 2020a. The effect and mechanism of La2O3 on the anti-ultraviolet aging characteristics of virgin bitumen. Constr Build Mater 230, 116967.
Jiang, W., Yuan, D., Shan, J., Ye, W., Lu, H., Sha, A., 2020b. Experimental study of the performance of porous ultra-thin asphalt overlay. International Journal of Pavement

Engineering, 1-13.
Jing, R., Varveri, A., Liu, X., Scarpas, A., Erkens, S., 2019a. Ageing effect on chemo-mechanics of bitumen. Road Mater Pavement, 1-16.
Jing, R., Varveri, A., Liu, X., Scarpas, A., Erkens, S., 2019b. Laboratory and Field Aging Effect on Bitumen Chemistry and Rheology in Porous Asphalt Mixture. Transport Res Rec 2673(3), 365-374.
Liu, H., Sha, A., Tong, Z., Gao, J., 2018. Autonomous microscopic bunch inspection using region-based deep learning for evaluating graphite powder dispersion. Constr Build Mater 173, 525-539.
Liu, X., Li, T., Zhang, H., 2018. Short-term aging resistance investigations of polymers and polyphosphoric acid modified asphalt binders under RTFOT aging process. Constr Build Mater 191, 787-794.
Luo, S., Tian, J., Liu, Z., Lu, Q., Zhong, K., Yang, X., 2020. Rapid determination of styrene-butadiene-styrene (SBS) content in modified asphalt based on Fourier transform infrared (FTIR) spectrometer and linear regression analysis. Measurement 151, 107204.
Marsac, P., Piérard, N., Porot, L., Grenfell, J., Mouillet, V., Pouget, S., Besamusca, J., Farcas, F., Gabet, T., Hugener, M., 2014. Potential and limits of FTIR methods for reclaimed asphalt characterisation. Mater Struct 47(8), 1273-1286.
Mazumder, M., Ahmed, R., Ali, A.W., Lee, S.-J., 2018. SEM and ESEM techniques used for analysis of asphalt binder and mixture: A state of the art review. Constr Build Mater 186, 313-329.
Mousavi, M., Pahlavan, F., Oldham, D., Hosseinnezhad, S., Fini, E.H., 2016. Multiscale investigation of oxidative aging in biomodified asphalt binder. The Journal of Physical Chemistry C 120(31), 17224-17233.
Osmari, P.H., Leite, L.F.M., Aragão, F.T.S., Cravo, M.C.C., Dantas, L.N., Macedo, T.F., 2019. Cracking resistance evaluation of asphalt binders subjected to different laboratory and field aging conditions. Road Mater Pavement 20(sup2), S663-S677.
Qin, X.T., Zhu, S.Y., He, X., Jiang, Y., 2018. High temperature properties of high viscosity asphalt based on rheological methods. Constr Build Mater 186, 476-483.
Singh, B., Kumar, P., 2019. Effect of polymer modification on the ageing properties of asphalt binders: Chemical and morphological investigation. Constr Build Mater 205, 633-641.
Stempihar, J., Gundla, A., Underwood, B.S., 2018. Interpreting stress sensitivity in the multiple stress creep and recovery test. J Mater Civil Eng 30(2), 04017283.
Sun, D., Zhang, L., Zhang, X., 2011. Quantification of SBS Content in SBS Polymer Modified Asphalt by FTIR, in: Bu, J.L., Wang, P.C., Ai, L., Sang, X.M., Li, Y.G. (Eds.), Applications Of Engineering Materials, Pts 1-4. pp. 953-+.
Wang, F., Zhang, L., Zhang, X., Li, H., Wu, S., 2020. Aging Mechanism and Rejuvenating Possibility of SBS Copolymers in Asphalt Binders. Polymers-Basel 12(1), 92.
Wang, H., Ma, Z., Chen, X., Hasan, M.R.M., 2020. Preparation process of bio-oil and bio-asphalt, their performance, and the application of bio-asphalt: a comprehensive review. Journal of Traffic and Transportation Engineering (English Edition).
Wang, J., Yuan, J., Kim, K.W., Xiao, F., 2018. Chemical, thermal and rheological characteristics of composite polymerized asphalts. Fuel 227, 289-299.
Wang, W., Jia, M., Jiang, W., Lou, B., Jiao, W., Yuan, D., Li, X., Liu, Z., 2020. High temperature property and modification mechanism of asphalt containing waste engine oil bottom. Construction and Building Materials 261, 119977.

Wu, Y., 2017. Low-temperature rheological behavior of ultraviolet irradiation aged matrix asphalt and rubber asphalt binders. Constr Build Mater 157, 708-717.
Xia, T., Qin, Y., Xu, J., Zhou, L., Chen, W., Dai, J., 2018. Viscoelastic phase separation and crystalline-to-amorphous phase transition in bitumen/SBS/PE blends. Polymer 155, 129-135.
Xu, O., Xiao, F., Amirkhanian, S.N., Liu, Y., Han, S., 2016. Long-term aging effect on rheological properties of combined binders from various polymers with ground tire rubber. Canadian Journal of Civil Engineering 43(5), 451-460.
Ye, W., Jiang, W., Li, P., Yuan, D., Shan, J., Xiao, J., 2019. Analysis of mechanism and time-temperature equivalent effects of asphalt binder in short-term aging. Constr Build Mater 215, 823-838.
Yourong, T., Zhang, H., Cao, D., Xia, L., Du, R., Shi, Z., Dong, R., Wang, X., 2019. Study on cohesion and adhesion of high-viscosity modified asphalt. International Journal of Transportation Science and Technology 8(4), 394-402.
Yuan, Y., Zhu, X., Chen, L., 2020. Relationship among cohesion, adhesion, and bond strength: From multi-scale investigation of asphalt-based composites subjected to laboratory-simulated aging. Materials & Design 185, 108272.
Zhang, F., Hu, C., 2017. Preparation and properties of high viscosity modified asphalt. Polymer Composites 38(5), 936-946.
Zhang, F., Hu, C., Zhuang, W., 2018. The research for low-temperature rheological properties and structural characteristics of high-viscosity modified asphalt. J Therm Anal Calorim 131(2), 1025-1034.

Author biographies and photos

Wei Jiang, PhD, is currently serving as the professor in Chang'an University, and has engaged in teaching and research work in the field of road engineering. His research fields include: design and construction of eco-friendly functional road materials, future-oriented smart road materials, collaborative design of pavement material performance and function method, etc. He has published at least 70 papers on international and Chinese academic journals.

Dongdong Yuan is a PhD candidate in the Department of Road and Railway Engineering at Chang'an University. His research focuses on thermoelectric asphalt pavement and modified asphalt. He received his B.S. degree in traffic engineering from Qingdao University of Technology, China in 2015 and his M.S. degree in transportation engineering from Chang'an University, China in 2018.

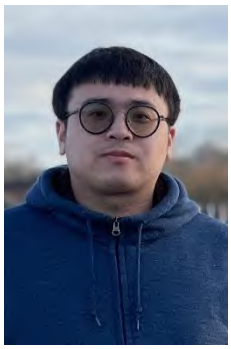

Zheng Tong received his B.S. degree in civil engineering from Northeast Forestry University, China in 2015 and his M.S. degree in transportation engineering from Chang'an University, China in 2018. His research interests concern pattern recognition, deep learning, and the application of belief function.

Aimin Sha, PhD, is currently serving as the professor in Chang'an University, and has engaged in teaching and research work in the field of road engineering more than 20 years. His research fields include: multi-index design method of semi-rigid base, modern eco-friendly pavement construction technology, construction quality control system of asphalt pavement, construction technology of smart road, etc. He has published more than 260 papers on international and Chinese academic journals.

Jingjing Xiao, PhD, is currently serving as the associate professor in Chang'an University, and has engaged in teaching and research work in the field of building materials and structure. Her research fields include: design of low emission pavement materials, performance of recycled pavement materials, eco-friendly functional road materials, etc. She has published at least 30 papers on international and Chinese academic journals.

Meng Jia is a PhD candidate in the Department of Road and Railway

Engineering at Chang'an University. His research focuses on asphalt modification technology and intelligent road materials. He has published at least 7 articles in internationally renowned journals.

Wanli Ye is a PhD candidate in the School of Transportation Science and Engineering at Harbin Institute of Technology. His research interests include studies on 3D reconstruction, machine learning, building materials, tire-pavement contact, non-destructive testing, full life cycle, waste materials recycling, and pollution/emission minimizing. He earned his bachelor's degree in Civil Engineering from Zhejiang Sci-tech University, PR China, and master's degree in Highway and Railway Engineering from Chang'an University, PR China.

Wentong Wang is a PhD candidate in the Department of Road and Railway Engineering at Chang'an University. His research focuses on studies related to solving applied and practical problems related to transportation engineering. His research interests include studies on self-luminous road intelligent materials, asphalt modification and regeneration technology.